5th Joint International Symposium on Deformation Monitoring (JISDM), 20-22 June 2022, Valencia, Spain
DOI: http://doi.org/10.4995/JISDM2022.2022.13826

Imaging land subsidence in the Guadalentín River Basin (SE Spain) using Advanced Differential SAR Interferometry

Guadalupe Bru[1], Juan J. Portela[2], Pablo Ezquerro[1], M. Inés Navarro[3], Alejandra Staller[2], Marta Béjar-Pizarro[1], Carolina Guardiola-Albert[1], José A. Fernández-Merodo[1], Juan López-Vinielles[1], Roberto Tomás[3], Juan M. López-Sánchez[4]

[1] Instituto Geológico y Minero de España (IGME, CSIC). Calle de Ríos Rosas 23, 28003 Madrid, Spain, (g.bru@igme.es; p.ezquerro@igme.es; c.guardiola@igme.es; m.bejar@igme.es; jose.fernandez@igme.es; j.lopez@igme.es)
[2] Universidad Politécnica de Madrid, RG Terra: Geomatics, Natural Hazards and Risks, C/ Mercator 2, 28031 Madrid, Spain, (jj.portela@upm.es; a.staller@upm.es)
[3] Departamento de Ingeniería Civil, Universidad de Alicante, Carr. de San Vicente del Raspeig s/n, 03690 San Vicente del Raspeig, Spain, (mainnahe@ua.es; roberto.tomas@ua.es)
[4] Instituto Universitario de Investigación Informática, Universidad de Alicante, Carr. de San Vicente del Raspeig s/n, 03690 San Vicente del Raspeig, Spain, (juanma.lopez@ua.es)

Key words: *aquifer overexploitation; subsidence; P-SBAS; GNSS; Guadalentín River Basin*

ABSTRACT

Aquifer overexploitation can lead to the irreversible loss of groundwater storage caused by the compaction or consolidation of unconsolidated fine-grained sediments resulting in land subsidence. Advanced Differential SAR Interferometry (A-DINSAR) is particularly efficient to monitor progressive ground movements, making it an appropriate method to study depleting aquifers undergoing overexploitation and land subsidence. The Guadalentín River Basin (Murcia, Spain) is a widely recognized subsiding area that exhibits the highest rates of groundwater-related land subsidence recorded in Europe (>10 cm/yr). The basin covers an extension of more than 500 km^2 and is underlain by an overexploited aquifer-system formed by two contiguous hydraulically connected units (Alto Guadalentín and Bajo Guadalentín). Although during the last years the piezometric levels have partially stabilized, the ongoing aquifer-system deformation is evident and significant, as revealed by the A-DInSAR analysis presented. In this work, we submit the first vertical and horizontal (E-W) decomposition results of the LOS velocity and displacement time series of the whole Guadalentín Basin obtained from two datasets of Sentinel-1 SAR acquisitions in ascending and descending modes. The images cover the period from 2015 to 2021 and they were processed using the Parallel Small BAseline Subset (P-SBAS) implemented by CNR-IREA in the Geohazards Exploitation Platform (GEP) on-demand web tool, which is funded by the European Space Agency. The output ascending and descending measurement points of P-SBAS lie on the same regular grid, which is particularly suited for the geometrical decomposition. Time series displacements are compared to a permanent GNSS station located in the Bajo Guadalentín basin.

I. INTRODUCTION

Aquifer overexploitation can lead to the irreversible loss of groundwater storage caused by the compaction or consolidation of unconsolidated fine-grained sediments, resulting in land subsidence. The displacement is mainly downward, though associated horizontal deformation often has significant damaging effects (Galloway and Burbey, 2011). Advanced Differential SAR Interferometry (A-DInSAR) is particularly efficient to monitor progressive ground movements, making it an appropriate method to study depleting aquifers undergoing overexploitation and land subsidence. Traditionally, in land subsidence studies it was assumed that the ground surface deformation obtained from A-DInSAR corresponds only to vertical deformation, but the availability of ascending and descending SAR satellites orbits allows decomposing the LOS mean velocity and displacements into vertical and east-west components. The north-south remains unknown due to the quasi polar orbit of the satellites (Cigna and Tapete, 2021a; Fernandez *et al.*, 2018).

The Guadalentín River Basin (Murcia, Spain) is a widely recognized subsiding area that exhibits the highest rates of groundwater-related land subsidence recorded in Europe, reaching values over 10 cm/yr (González and Fernández, 2011). There are several studies that have used multi-sensor SAR images from ERS, ENVISAT, ALOS, Cosmo-SkyMed (CSK) and Sentinel-1 (S-1) satellites combined with GNSS measurements to study land subsidence in this area, however most of them have focused in the Alto Guadalentín aquifer (Béjar-Pizarro *et al.*, 2016; Bonì *et al.*, 2015; Ezquerro *et al.*, 2020; Fernandez *et al.*, 2018). In this work, we have measured land subsidence of the

whole Guadalentín Basin for the 2015-2021 period using S-1 data, and we have produced, for the first time, a vertical and horizontal (E-W) deformation map of the entire basin, calculated from ascending and descending orbit geometry decomposition. The A-DInSAR processing has been run in a cloud computing server, the Geohazards Exploitation Platform (GEP).

The deformation results have been validated with GNSS data, by projecting the three components into the ascending and descending geometry, and have been compared to previous studies.

II. Study Area

The Guadalentín River Basin is located in the province of Murcia (SE Spain) within a NE-SW elongated alpine orogenic tectonic depression of the Betic Cordillera. It has an extension of more than 500 km^2 and underneath there is an overexploited aquifer-system formed by two contiguous hydraulically connected units: Alto Guadalentín and Bajo Guadalentín aquifers (Figure 1). The basement of the basin is formed by Paleozoic metamorphic rocks with a horst and graben pattern, overlined by Miocene detrital deposits of conglomerates and calcarenites. The top of the sequence is constituted by Plio-Quaternary detrital and alluvial materials (*i.e.* conglomerates, sand, silt, and clay) deposited by the Guadalentín ephemeral river (Cerón and Pulido-Bosch, 1996). In some areas of the basin the Plio-Quaternary layer can be split into two sublayers: compressible soft soils in the upper most part and coarse fraction materials at the bottom (Béjar-Pizarro *et al.*, 2016; Bonì *et al.*, 2015). The coarse fraction of the Plio-Quaternary and the upper part of the Miocene are permeable. Therefore, the aquifer system can be considered as unconfined, consisting of two zones, an upper free layer and a lower layer semi-confined by the upper one and with the possibility of changing its state depending on the position of the piezometric surface (CHS, 2005). Nowadays, the Plio-Quaternary unconfined aquifer zone is almost drained, being the semi-confined Miocene the most productive zone.

The absence of permanent watercourses or positive transferences from other aquifer-systems makes the Guadalentín aquifer recharge almost limited to rainfall and watering returns (Ezquerro *et al.*, 2017). Considering the semi-arid climate of the region, with average annual precipitation of less than 250 mm for the last 20 years, it can be stated that the lowering of the groundwater level is strongly dependent on the extractions. The aquifer system has been extensively exploited for agricultural irrigation since the 1960's, causing an spatially heterogeneous decline in the aquifer-system levels of about 200 m in 50 years (Bonì *et al.*, 2015). The aquifer was declared officially overexploited in 1987 (IGME, 1997) and currently is in a state of quantitative disrepair due to overexploitation (CHS, 2021). Previous studies have established that there is relationship between groundwater changes and land subsidence on the entire Guadalentín aquifer-system (González and Fernández, 2011; Rigo *et al.*, 2013) and on the Alto Guadalentín basin (Bonì *et al.*, 2015; Ezquerro *et al.*, 2017; Ezquerro *et al.*, 2020; Fernández-Merodo *et al.*, 2021; Fernandez *et al.*, 2018).

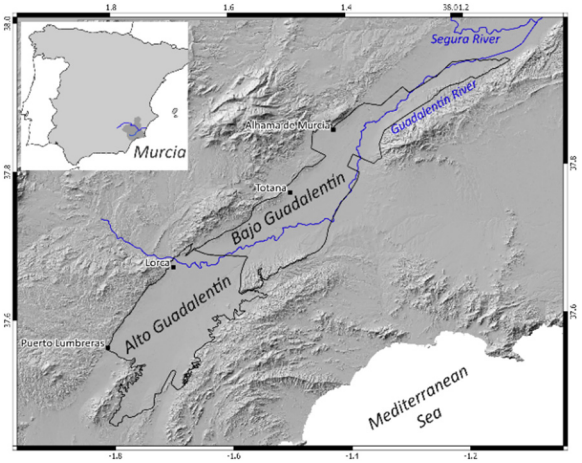

Figure 1. Location of the study area. Aquifers borders, rivers and main municipalities are shown.

III. Materials an Data

A. *SAR data and A- DInSAR processing*

The S-1 mission from the European Space Agency (ESA) comprises a constellation of two polar-orbiting SAR satellites operating at C-band. In this study, two S-1 datasets acquired between March 2015 and June 2021 in ascending and descending orbit modes were used (Table 1). The minimum revisit period of the constellation over the site is 6 days. We selected 182 S-1 SAR images in ascending mode and 176 in descending, with an average frequency of 12 days.

Table 1. A-DInSAR data parameters

Data	Parameters	
Orbit mode	Ascending	Descending
Track	103	8
Number of images	182	176
Initial date	2015-03-05	2015-02-27
End date	2021-06-07	2021-06-07
DS per km^2	150	150
LOS velocity range [cm/yr]	-7.3 to 1.6	-6.9 to 1.9
LOS velocity standard deviation	0.58	0.52

The multitemporal A-DInSAR analysis was performed using the Parallel computing solution of the Small BAseline Subset (P-SBAS) approach (Berardino *et al.*, 2002; Casu *et al.*, 2014; Manunta *et al.*, 2019) which was run in GEP (Foumelis *et al.*, 2019). The GEP is an on-demand web service funded by ESA, where A-DInSAR algorithms and computational resources are located together with the SAR data archives (De Luca *et al.*, 2015). Most of the parameters of the processing are settled automatically and have proven suitable in other land subsidence studies (Cigna and Tapete, 2021b). The

P-SBAS utilizes a small baseline interferogram arrangement, where a dense network is created linking multiple SAR images (Multi-master). It is a coherence-based method suited to Distributed Scatters (DS), *i.e.*, terrain patches whose scatter properties are not altered with time. The coherence estimation requires a spatial average within a two-dimension window, usually named as multilook (ML), which allows to reduce noise at the expenses of a spatial resolution loss (Mestre-Quereda *et al.*, 2018). P-SBAS applies a ML of 5 x 20 (azimuth x range) which generates DS of approximately 90 x 90 m size. The coherence threshold limits the selection of pixels above the specified coherence value, which was set to 0.70. The reference point was placed in the stable mountainous areas that surround the basin, although the algorithm automatically refines it and selects the one with best coherence conditions close to the one selected by the user. Moreover, at the end of the processing, the algorithm implements an average reference on the whole scene to avoid the dependence to one single point. The P-SBAS outputs for the individual S-1 ascending and descending processing were two data points or DS maps (Figure 2). Each data point contains geographical location, mean LOS velocity, LOS displacement time series, and the components of LOS unit vector along the north, east and vertical directions. These unit vectors depend on the ground track of the satellite flight direction and on the radar antenna incidence angle, which varies from the near to the far range of the SAR scene. Both datasets were cropped to an area of interest of 3,000 km^2 that covers completely the Guadalentín River Basin and contains a point density of 150 DS per km^2 in the two of them. The mean LOS velocities range from -7.3 to 1.6 cm/yr for the ascending orbit dataset and from -6.9 to 1.9 cm/yr for the descending orbit dataset. Negative and positive values indicate movement away and towards the satellite, respectively. The time series LOS displacement trends in Alto Guadalentín maximum deformation areas, both in ascending and descending orbit, are linear. The piezometric levels in this area have remained stable since 2009, with slight seasonal variations as a consequence of the rainfall regime and the irrigation seasons (CHS, 2021). In Bajo Guadalentín the displacement time series also have a linear trend with slight fluctuations in the maximum deformation area near Alhama de Murcia, where the piezometric levels have a deepening tendency since 2008 until the last measures taken in 2019 (CHS, 2021).

B. *GNSS Data*

A permanent GNSS station named ALHA is located within the Bajo Guadalentín Basin (Figure 2). It is installed in the municipality of Alhama de Murcia and belongs to the REGAM regional network (https://sitmurcia.carm.es/estaciones). It has been active since 2010. The daily RINEX observation files (GPS+GLONASS) of the ALHA station have been processed using Bernese 5.2 software (Dach *et al.*, 2015). We performed a static and relative processing (alongside other permanent GNSS stations in the region) to obtain a daily positioning solution referred to the ITRF2014 reference frame. Then, the horizontal tectonic plate movement was subtracted from the GNSS east and north components, after computing the predicted motion in ALHA with the Euler Pole defined for the region (Echeverria *et al.*, 2013). The displacement time series in the three components (*i.e.* east, north and up) for the same time period as the P-SBAS processing are represented in Figure 3. The resulting horizontal velocity is rather small, particularly in the north direction (~-0.7 mm/yr) when compared to the east direction (~2.3mm/yr). The subsiding vertical movement is moderate at this site (~-3.6 mm/yr).

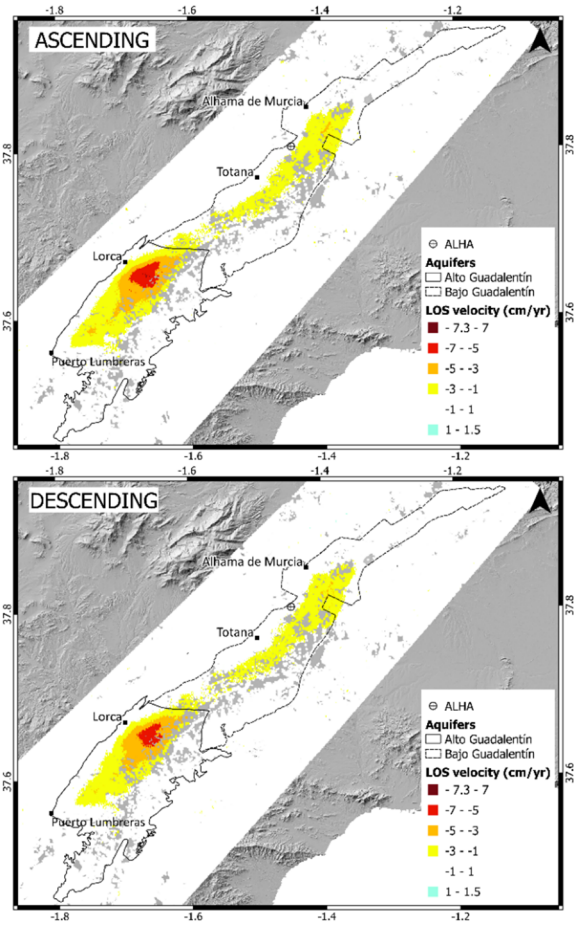

Figure 2. LOS mean velocity maps for the ascending (upper) and descending (bottom) S-1 datasets. Note magnitude is cm/yr.

IV. Methods

A. *Vertical and horizontal projection of SAR data*

We calculated the 2-D deformation field (eastward and vertical motion) from A-DInSAR results combining the two different viewing geometries of the ascending and descending satellite orbit passes, and assuming that the north component is negligible. This assumption is based on previous GNSS studies (Ezquerro *et al.*, 2020; Fernandez *et al.*, 2018) and on the ALHA station

measurements stated in previous section. The P-SBAS measurement points output lie on the same regular grid, both in ascending and descending datasets, which is particularly suited for the geometrical decomposition. We geographically intersected the DS points and calculated for each of them the vertical and east-west velocity, using Equations 1 and 2 (Béjar-Pizarro *et al.*, 2017). The DS that did not intersect the other orbit were discarded. The calculations were performed with the vector calculator tool of the open source software Q-GIS.

$$V_{east-west} = \frac{\left(\frac{vLOS_d}{H_d} - \frac{vLOS_a}{H_a}\right)}{\frac{E_d}{H_d} - \frac{E_a}{H_a}} \quad (1)$$

$$V_{vertical} = \frac{\left(\frac{vLOS_d}{E_d} - \frac{vLOS_a}{E_a}\right)}{\frac{H_d}{E_d} - \frac{H_a}{E_a}} \quad (2)$$

where H_d, H_a = vertical directional cosine of descending and ascending LOS unit vector
E_d, E_a = East-West directional cosine of descending and ascending LOS unit vector
$vLOS_d, vLOS_a$ = mean velocity in the Line Of Sight (LOS) of the descending and ascending satellite orbit modes

B. *Projection of GNSS data in LOS*

The GNSS displacement time series were smoothed using a moving average window of 12 days. Then, to compare the displacement time series from both monitoring techniques, we projected the three displacement components of the GNSS data into the ascending and descending LOS vectors using Equation 3.

$$d_{LOS} = d_{E-W} \cdot E + d_{N-S} \cdot N + d_v \cdot H \quad (3)$$

where d_{E-W}, d_{N-S}, d_v = east-west, north-south and vertical GNSS displacements
E, N, H = east-west, north-south and vertical LOS unit vectors at the location of the GNSS station

C. *Validation and comparison methodology*

The displacement time series obtained with P-SBAS and GNSS overlap for the whole period. We quantitatively compare the GNSS data projected in both ascending and descending LOS with the corresponding P-SBAS results, by means of the root mean squared error (RMSE) and the relative error, which is the percentage of RMSE with respect to the accumulated deformation, as in Ezquerro *et al.* (2020). The P-SBAS time series are computed as the average of the monitoring points (DS) contained in a 200 m radius buffer around the ALHA GNSS station.

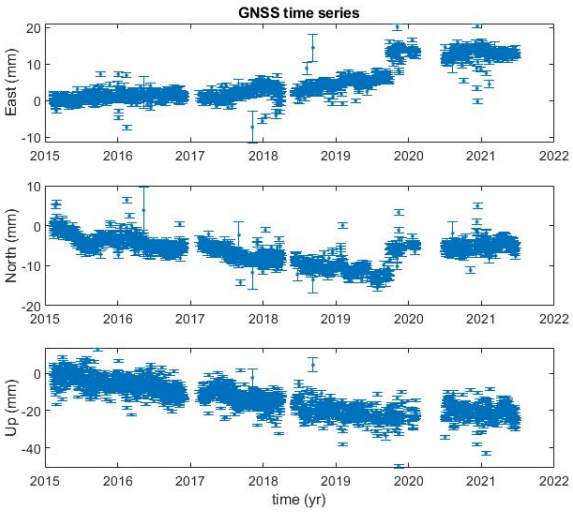

Figure 3. GNSS displacement time series at ALHA permanent station for the east, north and up components during the period 2015-2021. The error bars represent the uncertainties in the position. Note magnitude is mm.

V. Results

We have retrieved a complete picture of the Guadalentín River Basin spatial deformation for the period 2015-2021 in the vertical and horizontal (E-W) components, by the combination of ascending and descending SAR data (Figure 4). The sign criteria for the vertical component are negative values indicating downlift movement and positive uplift. In the case of the horizontal component, positive values indicate movement towards east and negative towards west. The vertical deformation concentrates along the central part of the Guadalentín valley, reaching up to -8.7 cm/yr in the north-western section of the Alto Guadalentín, near the city of Lorca. The vertical projection highlights an elongated down lift area towards Puerto Lumbreras that was not evident in the LOS mean velocity maps. The Bajo Guadalentín has lower vertical rates, reaching up to -5 cm/yr in the northern part of the Basin, where the industrial park of Alhama de Murcia is located. Horizontal E-W deformation magnitude in the Guadalentín River Basin is much lower than the vertical, ranging between -1.5 and 1.5 cm/yr, which is near the stable magnitude of 0.7 cm/yr considered, based on standard LOS deviation values. It is mainly detected in the left side of the Alto Guadalentín, with direction towards the east. At the right side of the basin, the pixel density is lower due to less temporal coherence and there are scarce DS indicating movement towards west.

Figure 5 plots the averaged ascending and descending P-SBAS time series within a 200 meters buffer from the ALHA station, along with the GNSS time series projected in the ascending and descending LOS geometry (that were previously smoothed and with the horizontal tectonic plate motion removed as explained above). The RMSE and its relative weight regarding the measured deformation (*i.e.* the relative error) were computed for the common epochs between the GNSS and PSBAS time series (see Table 2). The P-SBAS and

GNSS time series trends are relatively consistent in all the dataset, even though the magnitude of the displacement at ALHA station is low and below the stability threshold. Thus, the RMSE of the validation is small (~4 mm for both geometries), but the relative error with respect to the measured movements is high, particularly for the descending geometry (Table 2).

Table 2. RMSE and relative error of the PSBAS-LOS deformation with respect to GNSS LOS-projected deformation in ALHA

Orbit mode	RMSE [mm]	Rel. error [%]
Ascending	4.3	23.4
Descending	3.7	54.0

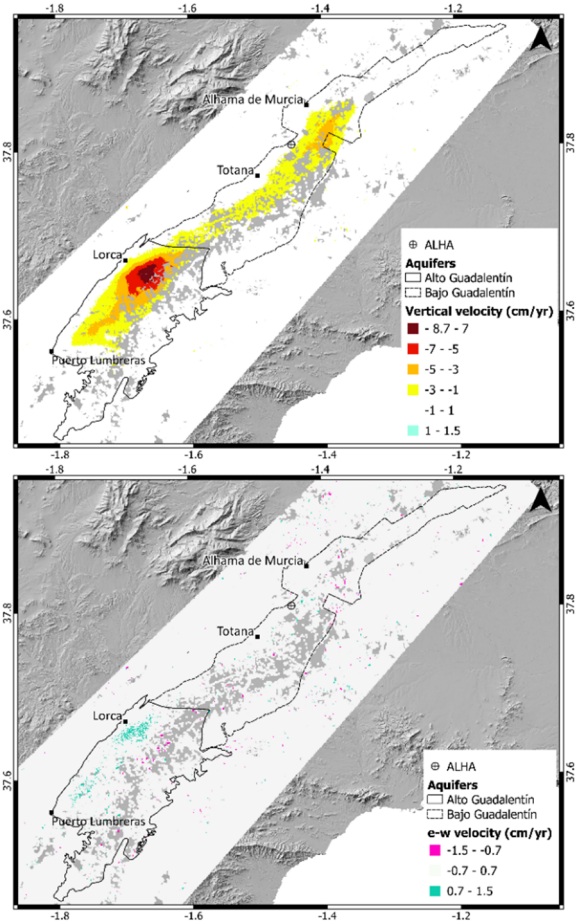

Figure 4. Mean velocity maps for the vertical (upper) and horizontal (bottom) components, projected from the S-1 ascending and descending datasets. Note velocity magnitude is in cm/yr.

VI. Discussion

The spatial deformation pattern obtained with the P-SBAS algorithm implemented in the GEP is in concordance with previous studies (Bonì *et al.*, 2015; Ezquerro *et al.*, 2020; Fernandez *et al.*, 2018), with maximum deformation areas located in the upper west side of Alto Guadalentín (south of the city of Lorca) and at the east of Alhama de Murcia in the Bajo Guadalentín. In previous works, the linear land subsidence displacements observed in the Alto Guadalentín until 2016 have been related to the residual compaction of the soft soil (Fernández-Merodo *et al.*, 2021), even though the piezometric levels remained stable. We observe the linear trend pattern in LOS is preserved for the presented studied period. Further investigations are needed to establish the relationship between Bajo Guadalentín land subsidence and piezometric fluctuations. The assumption of negligible north-south displacements is validated by GNSS data from previous studies in Alto Guadalentín for the period 2011-2018 (Ezquerro *et al.*, 2020). The GNSS stations used in that study were located in the maximum deformation area of Alto Guadalentín, whereas in the present study we use a GNSS station located in an area where the magnitude of displacements is very low. Despite this, the north horizontal velocity is rather small (~-0.7 mm/yr) when compared to the east direction (~2.3mm/yr), so we considered the premise valid.

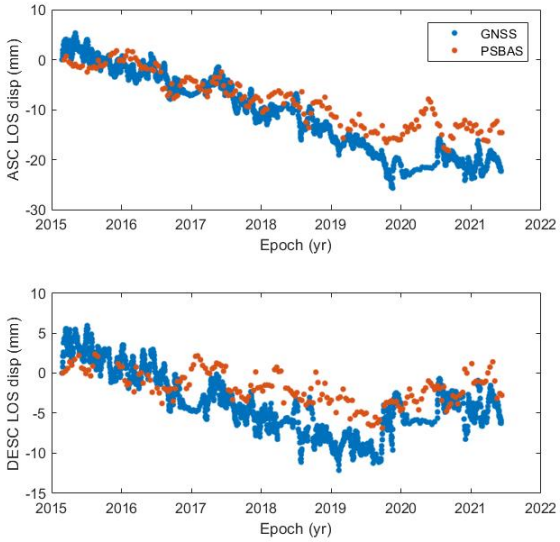

Figure 5. Comparison of the P-SBAS and GNSS time series in the LOS direction, at ALHA station, for ascending and descending orbits. Note displacement magnitude is in mm.

The projected P-SBAS velocities highlight the land subsidence spatial distribution and underscore the significance of horizontal displacements, especially in the Alto Guadalentín where rates are higher. The lower coherence at the right side of the valley can partially mask horizontal movements towards the west. On the contrary, horizontal motion towards east is evident in the right side of Alto Guadalentín where DS density is much higher. The magnitude of the horizontal rates in Alto Guadalentín are in concordance with the observations made by Fernandez *et al.* (2018) by means of GNSS campaigns (0.5–0.9 cm/yr) and S-1 data (1.0–1.5 cm/yr), and by Ezquerro *et al.* (2020) using S-1 and CSK data (0.7–1.5 cm/year), for the periods 2015-2017 and 2011-2016 respectively. Projected vertical velocities of those studies, up to -8 cm/yr and -7 cm/yr correspondingly, are also in the same order of magnitude that the present study.

It has to be considered that the rate of displacement at the ALHA location is below the order of P-SBAS stability threshold, that has been stablished as twice the standard LOS velocity deviation (1cm/yr). The temporal coherence values of the DS around ALHA station are higher than 0.88, which holds their reliability. The comparison between time series displacement of P-SBAS and GNSS in LOS shows in general a good agreement.

VII. Conclusions

This work presents for the first time vertical and horizontal (E-W) decomposition of the LOS velocity and displacement time series over the whole Guadalentín River Basin obtained from two datasets of S-1 SAR acquisitions in ascending and descending modes. The period studied spans for almost six years, from March 2015 to June 2021. The P-SBAS processing has been run in the GEP web service, where all the technical resources are external, which simplifies the processing of big datasets. Although the tool is unsupervised, which means that the processing chains run automatically in the server without user interaction, the P-SBAS results have proven to be robust in the Guadalentín River Basin, where magnitude and spatial distribution of the land subsidence is well known. Future works will include further validation with more GNSS stations located in the valley and other monitoring techniques, such as leveling.

VIII. Acknowledgements

This study has received funding in framework of the RESERVOIR project (Sustainable groundwater RESources managEment by integrating eaRth observation deriVed monitoring and flOw modelIng Results), funded by the Partnership for Research and Innovation in the Mediterranean Area (PRIMA) programme supported by the European Union (Grant Agreement 1924; https://reservoir-prima.org/).

The study has also been supported by the Grant FPU19/03929 (funded by MCIN/AEI/10.13039/501100011033 and by "FSE invests in your future"); the Project CGL2017-83931-C3-3-P (funded by MCIN/ AEI/10.13039/501100011033 and by "ERDF A way of making Europe"); the ESA-MOST China DRAGON-5 Project (ref. 59339) and the SARAI Project PID2020-116540RB-C22 (funded by MCIN/ AEI /10.13039/501100011033).

Copernicus Sentinel-1 IW SAR data were provided and processed in ESA's Geohazards Exploitation Platform (GEP), in the framework of the GEP Early Adopters Programme.

References

Béjar-Pizarro, M., Guardiola-Albert, C., García-Cárdenas, R. P., Herrera, G., Barra, A., López Molina, A., Tessitore, S., Staller, A., Ortega-Becerril, J. A., and García-García, R. P., (2016). Interpolation of GPS and geological data using InSAR deformation maps: Method and application to land subsidence in the alto guadalentín aquifer (SE Spain): *Remote Sensing*, v. 8, no. 11, p. 965.

Béjar-Pizarro, M., Notti, D., Mateos, R. M., Ezquerro, P., Centolanza, G., Herrera, G., Bru, G., Sanabria, M., Solari, L., and Duro, J., (2017). Mapping vulnerable urban areas affected by slow-moving landslides using Sentinel-1 InSAR data: *Remote Sensing*, v. 9, no. 9, p. 876.

Berardino, P., Fornaro, G., Lanari, R., and Sansosti, E., (2002). A new algorithm for surface deformation monitoring based on small baseline differential SAR interferograms: *Geoscience and Remote Sensing*, IEEE Transactions on, v. 40, no. 11, pp. 2375-2383.

Bonì, R., Herrera, G., Meisina, C., Notti, D., Béjar-Pizarro, M., Zucca, F., González, P. J., Palano, M., Tomás, R., and Fernández, J., (2015). Twenty-year advanced DInSAR analysis of severe land subsidence: The Alto Guadalentín Basin (Spain) case study: *Engineering Geology*, v. 198, pp. 40-52.

Casu, F., Elefante, S., Imperatore, P., Zinno, I., Manunta, M., De Luca, C., and Lanari, R., (2014). SBAS-DInSAR parallel processing for deformation time-series computation: IEEE Journal of Selected Topics in *Applied Earth Observations and Remote Sensing*, v. 7, no. 8, pp. 3285-3296.

Cerón, J., and Pulido-Bosch, A., (1996). Groundwater problems resulting from CO 2 pollution and overexploitation in Alto Guadalentín aquifer (Murcia, Spain). *Environmental Geology*, v. 28, no. 4, pp. 223-228.

Cigna, F., and Tapete, D., (2021a). Satellite InSAR survey of structurally-controlled land subsidence due to groundwater exploitation in the Aguascalientes Valley, Mexico. *Remote Sensing of Environment*, v. 254, p. 112254.

Cigna, F., and Tapete, D., (2021b). Sentinel-1 BigData Processing with P-SBAS InSAR in the Geohazards Exploitation Platform: An Experiment on Coastal Land Subsidence and Landslides in Italy. *Remote Sensing*, v. 13, no. 5, p. 885.

CHS, (2005). Asistencia técnica para el estudio de cuantificación del volumen anual de sobreexplotación de los acuíferos de la Unidad Hidrogeológica 07.28 Alto Guadalentín 07.33 Águilas.

CHS, (2021). Memoria Plan Hidrológico de la Demarcación del Segura 2022/2027. Ministerio para la Transición Ecológica y el Reto Demográfico.

Dach, R., Lutz, S., Walser, P., and Fridez, P., (2015). Bernese GNSS software version 5.2.

De Luca, C., Cuccu, R., Elefante, S., Zinno, I., Manunta, M., Casola, V., Rivolta, G., Lanari, R., and Casu, F., (2015). An on-demand web tool for the unsupervised retrieval of earth's surface deformation from SAR data: The P-SBAS service within the ESA G-POD environment. *Remote Sensing*, v. 7, no. 11, pp. 15630-15650.

Echeverria, A., Khazaradze, G., Asensio, E., Gárate, J., Dávila, J. M., and Suriñach, E., (2013). Crustal deformation in eastern Betics from CuaTeNeo GPS network. *Tectonophysics*, v. 608, pp. 600-612.

Ezquerro, P., Guardiola-Albert, C., Herrera, G., Fernández-Merodo, J. A., Béjar-Pizarro, M., and Bonì, R., (2017). Groundwater and subsidence modeling combining geological and multi-satellite SAR data over the alto guadalentín aquifer (SE Spain). *Geofluids*, v. 2017.

Ezquerro, P., Tomás, R., Béjar-Pizarro, M., Fernández-Merodo, J., Guardiola-Albert, C., Staller, A., Sánchez-Sobrino, J., and Herrera, G., (2020). Improving multi-technique monitoring using Sentinel-1 and Cosmo-SkyMed data and upgrading groundwater model capabilities. *Science of The Total Environment*, v. 703, p. 134757.

Fernández-Merodo, J., Ezquerro, P., Manzanal, D., Béjar-Pizarro, M., Mateos, R., Guardiola-Albert, C., García-Davalillo, J., López-Vinielles, J., Sarro, R., and Bru, G., (2021). Modeling historical subsidence due to groundwater withdrawal in the Alto Guadalentín aquifer-system (Spain). *Engineering Geology*, v. 283, p. 105998.

Fernandez, J., Prieto, J. F., Escayo, J., Camacho, A. G., Luzón, F., Tiampo, K. F., Palano, M., Abajo, T., Pérez, E., and Velasco, J., (2018). Modeling the two-and three-dimensional displacement field in Lorca, Spain, subsidence and the global implications. *Scientific reports*, v. 8, no. 1, p. 1-14.

Foumelis, M., Papadopoulou, T., Bally, P., Pacini, F., Provost, F., and Patruno, J., (2019). Monitoring Geohazards using on-demand and systematic services on Esa's Geohazards exploitation platform, in *Proceedings IGARSS 2019 IEEE International Geoscience and Remote Sensing Symposium2019*, IEEE, pp. 5457-5460.

Galloway, D. L., and Burbey, T. J., (2011). Regional land subsidence accompanying groundwater extraction. *Hydrogeology Journal*, v. 19, no. 8, pp. 1459-1486.

González, P. J., and Fernández, J., 2011, Drought-driven transient aquifer compaction imaged using multitemporal satellite radar interferometry. *Geology*, v. 39, no. 6, pp. 551-554.

IGME, (1997). Catálogo de acuíferos con problemas de sobreexplotación o salinización. Predefinición del programa de actuación: Segura, Ministerio de Medio Ambiente.

Manunta, M., De Luca, C., Zinno, I., Casu, F., Manzo, M., Bonano, M., Fusco, A., Pepe, A., Onorato, G., and Berardino, P., (2019). The parallel SBAS approach for Sentinel-1 interferometric wide swath deformation time-series generation: algorithm description and products quality assessment. *IEEE Transactions on Geoscience and Remote Sensing,* v. 57, no. 9, pp. 6259-6281.

Mestre-Quereda, A., Lopez-Sanchez, J. M., Ballester-Berman, J. D., Gonzalez, P. J., Hooper, A., and Wright, T. J., (2018). Evaluation of the Multilook Size in Polarimetric Optimization of Differential SAR Interferograms. *IEEE Geoscience and Remote Sensing Letters*, v. 15, no. 9, pp. 1407-1411.

Rigo, A., Béjar-Pizarro, M., and Martínez-Díaz, J., (2013). Monitoring of Guadalentín valley (southern Spain) through a fast SAR Interferometry method. *Journal of Applied Geophysics*, v. 91, pp. 39-48.